U.S. Department of Transportation

Federal Railroad Administration

Wheel Load Cycle Tag for Rail

Office of Research,
Development,
and Technology
Washington, DC 20590

DOT/FRA/ORD-15/39

Final Report
December 2015

NOTICE

This document is disseminated under the sponsorship of the Department of Transportation in the interest of information exchange. The United States Government assumes no liability for its contents or use thereof. Any opinions, findings and conclusions, or recommendations expressed in this material do not necessarily reflect the views or policies of the United States Government, nor does mention of trade names, commercial products, or organizations imply endorsement by the United States Government. The United States Government assumes no liability for the content or use of the material contained in this document.

NOTICE

The United States Government does not endorse products or manufacturers. Trade or manufacturers' names appear herein solely because they are considered essential to the objective of this report.

REPORT DOCUMENTATION PAGE

Form Approved
OMB No. 0704-0188

1. AGENCY USE ONLY (Leave blank)	2. REPORT DATE	3. REPORT TYPE AND DATES COVERED
	December 2015	Technical Report – April 2015

4. TITLE AND SUBTITLE
Wheel Load Cycle Tag for Rail

5. FUNDING NUMBERS

6. AUTHOR(S)
Mr. Lawrence Howarth (Principal Investigator), Mr. Erick Leiss, Mr. James Madera

7. PERFORMING ORGANIZATION NAME(S) AND ADDRESS(ES)
Navmar Applied Sciences Corporation
Advanced Acoustics Sector
607 Louis Drive STE G
Warminster, PA 18974

8. PERFORMING ORGANIZATION REPORT NUMBER
0025-15

9. SPONSORING/MONITORING AGENCY NAME(S) AND ADDRESS(ES)
U.S. Department of Transportation
Federal Railroad Administration
Office of Railroad Policy and Development
Office of Research, Development, and Technology
Washington, DC 20590

10. SPONSORING/MONITORING AGENCY REPORT NUMBER
DOT/FRA/ORD-15/39

11. SUPPLEMENTARY NOTES
COR: Cameron Stuart

12a. DISTRIBUTION/AVAILABILITY STATEMENT
This document is available to the public through the FRA Web site at http://www.fra.dot.gov.

12b. DISTRIBUTION CODE

13. ABSTRACT (Maximum 200 words)

The Federal Railroad Administration (FRA) has determined that there is a research need to collect and analyze statistical usage data to help ascertain the cumulative load-induced fatigue on rail track segments. The estimation of rail segment burdening through the determination of loaded or unloaded wheel passages is aided by obtaining totalized statistical counts that can serve as an early indication of potential track failures. This research focused on designing and extensively testing a small, self-powered track assessment gauge (TAG) device that was installed directly to the web of the track rail. This device was designed to tabulate train wheel passages and associate an “empty” or “loaded” status with passage of rolling trains. The measured statistical data was stored internally to the device and was field accessible for recovery via a non-contact hand-held unit. Additional testing is needed to confirm the actual power consumption during operation and sleep modes, and verify the operation and accuracy of the TAG unit in varied track/roadbed conditions.

14. SUBJECT TERMS
Rail fatigue, rail wear, rail traffic sensor, track, accelerometer, magnetometer, RFID / NFC

15. NUMBER OF PAGES
36

16. PRICE CODE

17. SECURITY CLASSIFICATION OF REPORT	18. SECURITY CLASSIFICATION OF THIS PAGE	19. SECURITY CLASSIFICATION OF ABSTRACT	20. LIMITATION OF ABSTRACT
Unclassified	Unclassified	Unclassified	

NSN 7540-01-280-5500
Standard Form 298 (Rev. 2-89)
Prescribed by ANSI Std. 239-18
298-102

METRIC/ENGLISH CONVERSION FACTORS

ENGLISH TO METRIC	METRIC TO ENGLISH
LENGTH (APPROXIMATE)	**LENGTH (APPROXIMATE)**
1 inch (in) = 2.5 centimeters (cm)	1 millimeter (mm) = 0.04 inch (in)
1 foot (ft) = 30 centimeters (cm)	1 centimeter (cm) = 0.4 inch (in)
1 yard (yd) = 0.9 meter (m)	1 meter (m) = 3.3 feet (ft)
1 mile (mi) = 1.6 kilometers (km)	1 meter (m) = 1.1 yards (yd)
	1 kilometer (km) = 0.6 mile (mi)
AREA (APPROXIMATE)	**AREA (APPROXIMATE)**
1 square inch (sq in, in^2) = 6.5 square centimeters (cm^2)	1 square centimeter (cm^2) = 0.16 square inch (sq in, in^2)
1 square foot (sq ft, ft^2) = 0.09 square meter (m^2)	1 square meter (m^2) = 1.2 square yards (sq yd, yd^2)
1 square yard (sq yd, yd^2) = 0.8 square meter (m^2)	1 square kilometer (km^2) = 0.4 square mile (sq mi, mi^2)
1 square mile (sq mi, mi^2) = 2.6 square kilometers (km^2)	10,000 square meters (m^2) = 1 hectare (ha) = 2.5 acres
1 acre = 0.4 hectare (he) = 4,000 square meters (m^2)	
MASS - WEIGHT (APPROXIMATE)	**MASS - WEIGHT (APPROXIMATE)**
1 ounce (oz) = 28 grams (gm)	1 gram (gm) = 0.036 ounce (oz)
1 pound (lb) = 0.45 kilogram (kg)	1 kilogram (kg) = 2.2 pounds (lb)
1 short ton = 2,000 pounds (lb) = 0.9 tonne (t)	1 tonne (t) = 1,000 kilograms (kg)
	= 1.1 short tons
VOLUME (APPROXIMATE)	**VOLUME (APPROXIMATE)**
1 teaspoon (tsp) = 5 milliliters (ml)	1 milliliter (ml) = 0.03 fluid ounce (fl oz)
1 tablespoon (tbsp) = 15 milliliters (ml)	1 liter (l) = 2.1 pints (pt)
1 fluid ounce (fl oz) = 30 milliliters (ml)	1 liter (l) = 1.06 quarts (qt)
1 cup (c) = 0.24 liter (l)	1 liter (l) = 0.26 gallon (gal)
1 pint (pt) = 0.47 liter (l)	
1 quart (qt) = 0.96 liter (l)	
1 gallon (gal) = 3.8 liters (l)	
1 cubic foot (cu ft, ft^3) = 0.03 cubic meter (m^3)	1 cubic meter (m^3) = 36 cubic feet (cu ft, ft^3)
1 cubic yard (cu yd, yd^3) = 0.76 cubic meter (m^3)	1 cubic meter (m^3) = 1.3 cubic yards (cu yd, yd^3)
TEMPERATURE (EXACT)	**TEMPERATURE (EXACT)**
[(x-32)(5/9)] °F = y °C	[(9/5) y + 32] °C = x °F

QUICK INCH - CENTIMETER LENGTH CONVERSION

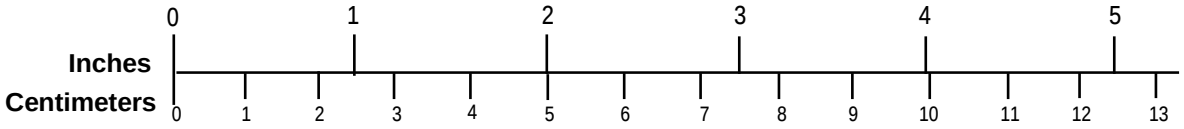

QUICK FAHRENHEIT - CELSIUS TEMPERATURE CONVERSIO

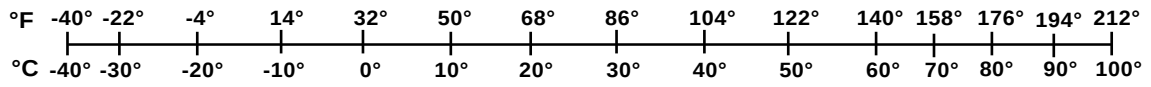

For more exact and or other conversion factors, see NIST Miscellaneous Publication 286, Units of Weights and Measures. Price $2.50 SD Catalog No. C13 10286

Updated 6/17/98

Acknowledgements

We would like to thank the New Hope and Ivyland Railroad (NHRR) and the Pennsylvania Northeastern Railroad (PN), who provided valuable track time to test our Wheel Load Cycle TAG sensor.

We would also like to thank Dr. Carlton Ho from the University of Massachusetts-Amherst for his insight and expertise, the Philadelphia Electric Trolley Museum, as well as Mr. Jim Fox Chief Control Center Officer Southeastern Pennsylvania Transportation Authority (SEPTA) their support in conducting this research.

Contents

Figures

Tables

Executive Summary

The Federal Railroad Administration (FRA) Research Initiative *Wheel Load Cycle Tag for Rail* identified the need for an autonomous device that records wheel loading in order to determine the service life of rail segments. To this end, Navmar Applied Sciences Corporation designed and fabricated a small, self-powered Track Assessment Gauge (TAG) then tested the device in the laboratory and at several field sites. This report documents Phase I of Advanced Acoustics Sector's (AAS) efforts to develop a sensor system capable of documenting wheel load events at Navmar.

We identified suitable sensors, developed an algorithm that detects wheel load events, and recommended a hybrid accelerometer-magnetometer sensor suite based on our research as well as our laboratory and field test results. Additionally, we were also able to verify collected data transfer to a non-contact, radio frequency (RF) handheld unit using Near Field Communication (NFC). However, additional testing is required to create a more robust pre-production prototype design.

Namur's Phase I TAG design was influenced by the following considerations:

- Low cost
- Small form factor
- Environmental ruggedness and durability
- Service life
- Energy harvesting potential (for system power augmentation)
- Easy rail installation
- Measurement accuracy
- Wireless data transfer from rail device to handheld RF unit

The initial TAG design implemented a pair of microchip-based, tri-axial accelerometers that were spaced at a fixed distance along the web of the rail so the device could exploit the signal difference or coherence between the adjacent sensors. Ultimately, this was a difficult goal to achieve while maintaining battery power and a small form factor.

Also, the processed accelerometer data that was collected provided an indication of loading, but conclusive and consistent wheel counting was unrealized. In concert with sensor development, research was conducted to implement the non-contact measurement data extraction via Radio Frequency Identification (RFID) techniques. Near Field Communication (NFC) was successfully used in lab-based tests to retrieve information stored on the TAG by employing a cell phone that was held in proximity to the unit.

Additional research with non-acoustic sensors yielded a small and low power magnetometer sensor that accurately indicated wheel passages during field testing, and the team identified a hybrid sensor suite system that used a magnetometer to identify and count the wheel passages combined with an accelerometer to provide relative loading indications. Additional development and testing is required to demonstrate that this combined hybrid sensor suite can simultaneously detect and accurately classify wheel loads.

Additional testing will be needed to confirm the actual power consumption during operation and sleep modes and verify the operation and accuracy of the TAG unit in varied track/roadbed conditions.

1. Introduction

The FRA's Research Initiatives for Rail Safety provides a metric of load-induced fatigue to predict rail longevity and potential safety concerns. By collecting usage statistics, in the form of a totalized count of wheel passage events and an estimation of rail segment burdening by the determination of loaded or unloaded wheel passages, increased safety can be achieved. As a result, the FRA requested that a measurement device be developed that is self-powered and consumed very low power, which reduces its dependence on external power supplies or recurring maintenance. In addition, unit cost, unit installation difficulty, expense and the expected operational lifetime of the device all dictated the final design methodology.

In order to minimize the workload associated with gathering the collected statistical data, it was essential to develop a simple technique for extracting recorded statistical information. RFID technology provided an ideal way to retrieve data without the dealing with the environmental concerns from contact-based data transfer, and it also allowed the RFID to power the TAG system with the radiated RF energy that is emitted while the stored data is downloaded to the reader.

The technology required to implement the envisioned system is well-established. Micro-electro-mechanical systems (MEMS), which are commonly found in our cell phones and game console controllers, are a mature technology and have dramatically driven down the cost of geophysical sensors and related measurement systems. These consumer applications have reduced the size and cost of digital three-axis accelerometers and field magnetometers, making them viable solutions for the measurement devices in the TAG system.

The developed concept can easily relocate and reuse the measurement systems, which offer a sizable reduction in the investment of materials and labor over permanent installations. It provides an inexpensive method for measuring and recording both track activity and relative loading events over extended periods of time, and its ease of installation allows the repositioning of the instrumentation to include multiple sites of strategic interest, and provide simultaneous information collection.

2. System Performance Requirements

The initial effort focused on the establishment of the system design requirements, specifically the required measurement parameters, the amount of data to be collected and stored, the download requirements and the necessary battery life. These requirements were based upon historical traffic density records, known physical characteristics of modern railroad equipment, anticipated signal processing requirements, and estimates of the system's power drain. Also, the team augmented their requirements development process by reviewing existing empirical data from prior experiments that involved train-induced track vibration. A flow chart of the system functional operation was developed, and it documented the standby, alert, transition from sleep, data collection, computation, and data retrieval modes (Figure 1).

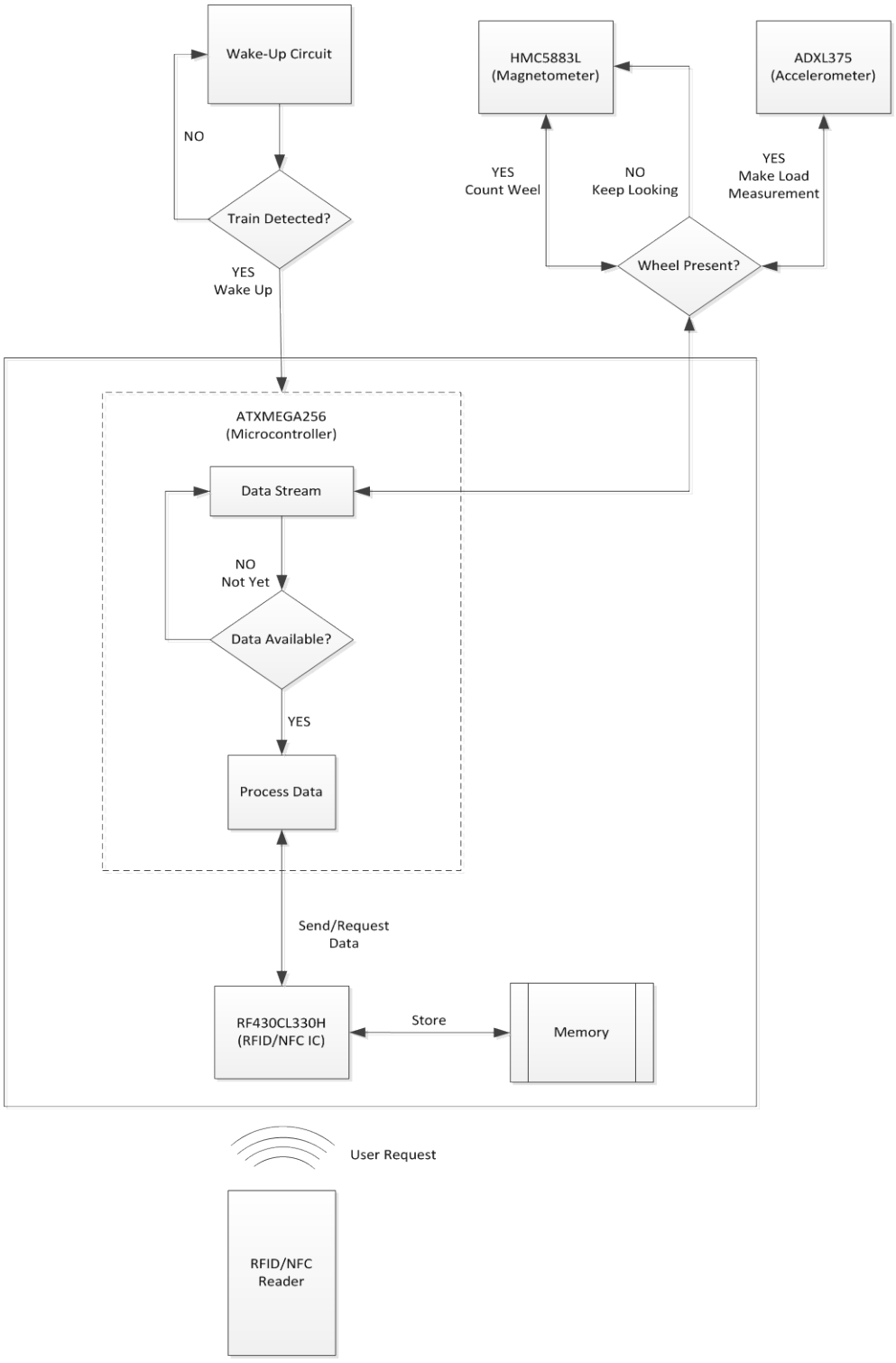

Figure 1. System Flow Chart

3. Preliminary System Development

3.1 Sensor System Development

In this measurement system, the exploitable vibrational signals generated by the interaction of the train wheels along the rail are used to determine instantaneous wheel positioning and conceive a relativistic load measurement of the passing train car. Analog Devices' ADXL345 and, later, the ADXL347 digital triaxial accelerometer were selected and tested on the merits of power consumption, performance, physical size, and cost.

3.1.1 Rail Mount

Several coupling methods were considered based on transfer of vibrational energy from the multi-directional oscillations of the rail to the measurement sensor. Experimentation was required to determine an effective method of attachment of the accelerometer to the rail, because the magnitude of vibrational energy generated by a passing train can vary significantly depending on how firmly the sensor and rail web are coupled.

The earliest and most basic configuration of the ADXL345 accelerometers consisted of an electrical interface board that was rigidly mounted between two aluminum plates. The aluminum plates served as protective covers and generated a load path for compression mounting to the rail web using a custom clamp fixture (Figure 2). A rare earth magnetic mount (also shown in Figure 2) was also utilized but the magnetic mounting was only for attachment expediency during testing.

Figure 2. Rigid and Magnetic Mounts for ADXL345 Accelerometer

The ADXL345 accelerometer has an input range of ±16g, which seemed sufficient during the design phase of the project. Initial data collection sets showed evidence of clipping during the time a train was passing over the sensors as shown in Figure 3, which indicated that the measured signal exceeded the range of the sensor. The team discussed concerns such as the recovery time from overloading conditions and the effects of out-of-band clipping on data of interest.

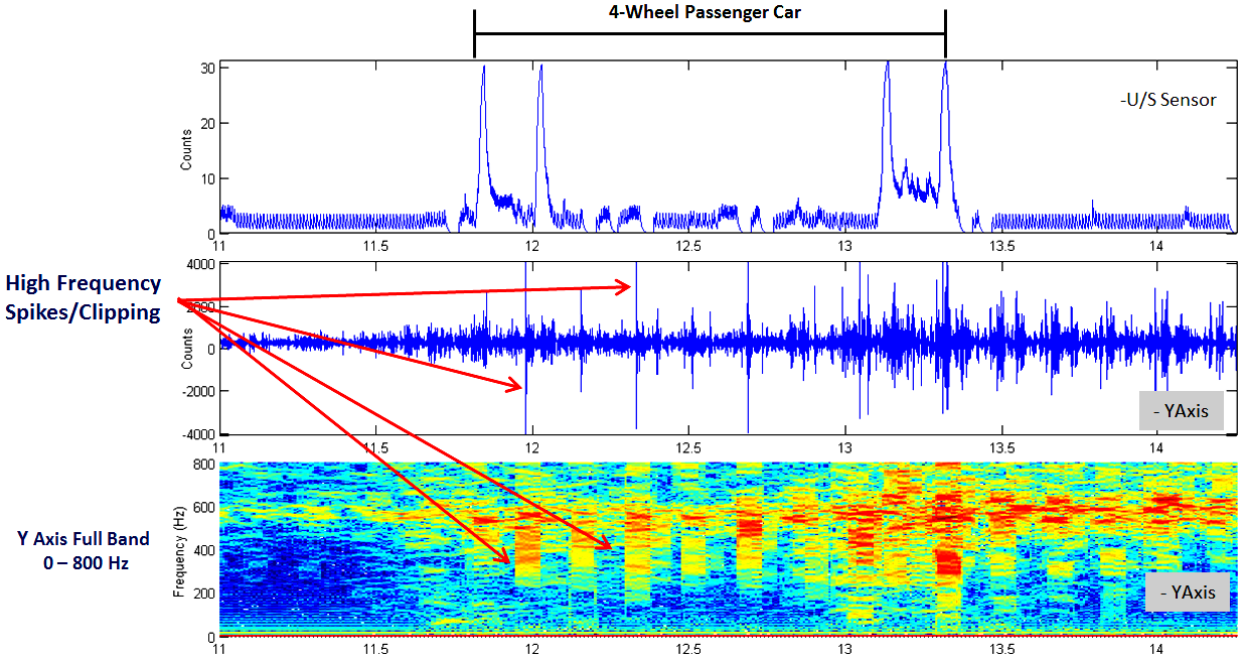

Figure 3. Vibration Overload (clipping) Recordings - Crestmont Station SEPTA Test#1

The possibility that potential signal aliasing would corrupt measurements of interest led to the team investigating simple mechanical approaches to decouple the sensor's high frequency mechanical interaction with the rail. Compliant members, which used materials such as rubber standoffs and low durometer foam pads, were applied between the mount and the sensor (Figure 4). Unfortunately, these new solutions led to concerns about the effects of materials aging and the materials' performances varying with temperature. During the course of these tests, the magnetic mounting configuration was the setup of choice because of its simplicity of attaching the test sensors to the rail.

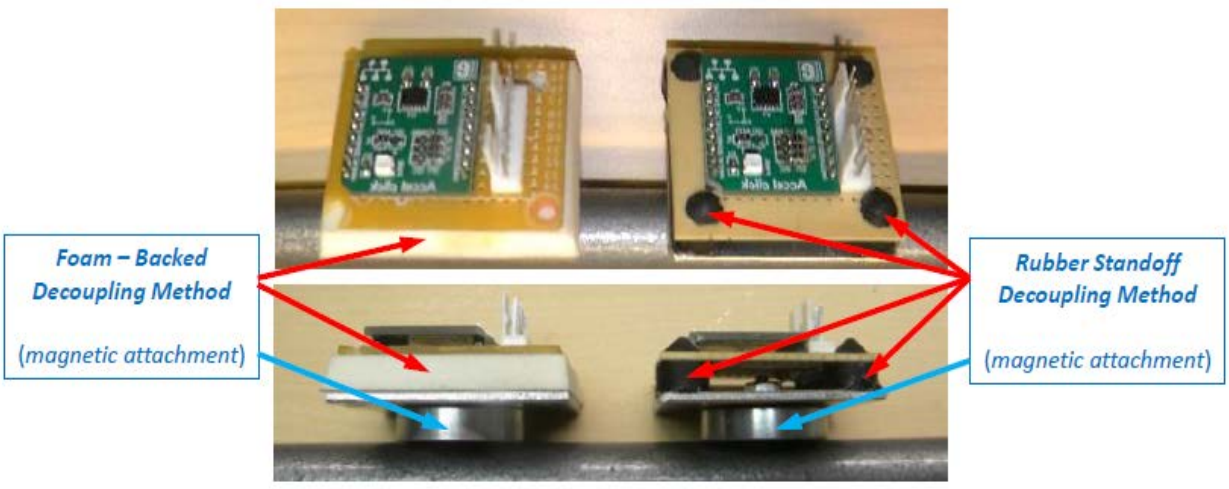

Figure 4. Implementation of Decoupling Materials

The decoupling methods described above did not completely remove the presence of clipping. At the suggestion of the project sponsor, a phone consultation was conducted with Dr. Carlton Ho of the University of Massachusetts, who specializes in studying ballast degradation and contamination. After talking with Dr. Ho, it was decided that experimentation with a higher input range accelerometer was essential to resolving the effects of signal clipping observed in the preliminary tests. Side-by-side comparisons of the data collected in the two accelerometer sensor ranges did not indicate a high degree of data contamination due to signal excess. Out-of-range signals were naturally truncated but adverse effects did not seem to permeate the non-clipped signals; this was verified by comparing the output from the higher input range accelerometer to the lower range unit. Then, focal emphasis was turned to displacement and deflection measurements on rail tie plates in addition to the rail web.

The ADXL375 high input range accelerometer was a direct replacement to the ADXL345, providing high resolution measurements of up to ±200g without change to the existing software embedded within the microcontroller. The mounting configuration for data collection with the new sensors returned to the previously used hard-coupled clamping mount so the system could measure higher frequencies and input levels. Subsequently, test configurations used both high and low input range sensors mounted magnetically to tie plates, along with sensors mechanically clamped to the rail foot, to investigate the phase differences between the displacement waveforms.

3.1.2 Software Program

The processor used in the TAG is the Atmel AVR AXMEGA A3BU, a low-cost device. The processor has five software selectable power saving modes which allows optimization of battery usage and functionality. In extended standby mode, both the main oscillator and the asynchronous timer continue to run, allowing the application to maintain a timer base while the rest of the device is sleeping. This allows very fast startup combined with low power consumption. The processor controls and handles the communications among the external components and also has direct control of the RF communications and on-board data storage.

System Architecture

The rapid growth of mobile computing and Wi-Fi enabled devices allowed the team to add wireless communication to our sensor package at a low cost. Near field communication (NFC) and radio-frequency identification (RFID) are subclasses of this technology that allow smartphones and smart-enabled handhelds/readers to establish radio communication with various devices for the purpose of data transfer.

Integrated into the unit's electronics is an ultra-low power NFC/RFID transponder IC from Texas Instruments (RF430CL330H). The transponder performs as the target in a two part wireless link initiated by a host. Once activated, small amounts of data can be transferred between the two devices when held in close proximity. Not only is this a non-contact method of transferring data, the transponder optimizes power management by scavenging RF energy emitted by the host, eliminating battery consumption during reading and writing to the chip's internal memory. Configuration information is handled through the NFC data exchange format (NDEF) message via the chip's SRAM, which is initialized during startup.

The RF430CL330H is an NFC Type 4B/ISO14443B dynamic and dual interface tag platform. The features include low cost NFC/RFID protocol using I2C or SPI interface to communicate with a parent micro control unit (MCU) at a maximum speed of up to 848kbps. The chip is compatible with 13.65MHz radio frequencies, and transfers NDEF messages to 3kb of internal SRAM at a distance of up to 30mm. The unique feature of this IC among other tags is its ability to be directly connected to a MCU to read, write, and re-write data. Figure 5 illustrates the selected NDEF message structure.

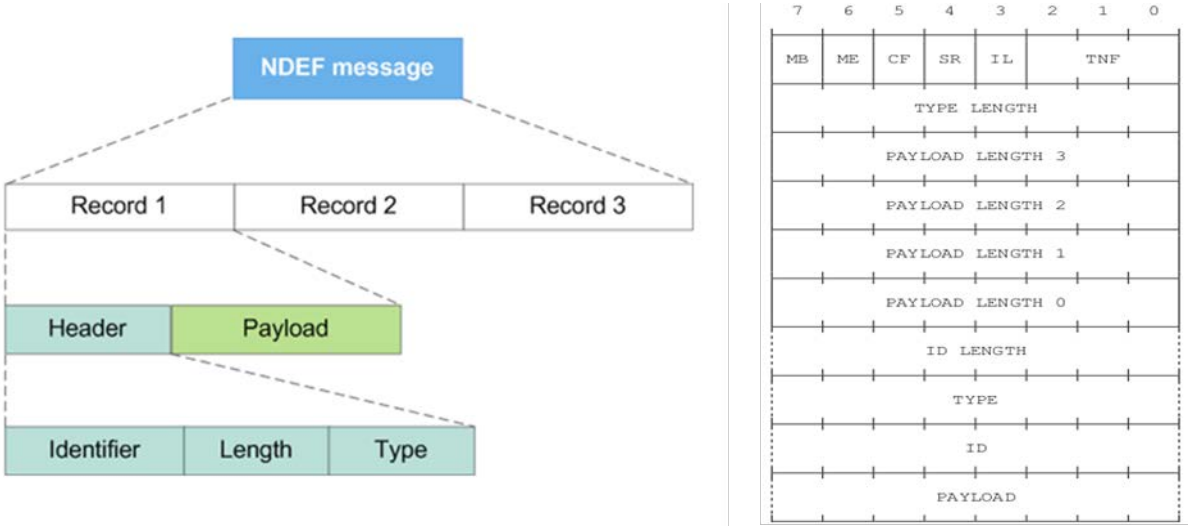

Figure 5. NDEF Message and Record Structure

To demonstrate non-contact data transmission, a prototype breadboard was constructed in the lab with the RF430CL330H evaluation platform and the Atmel XMEGA-A3BU demonstration kit (Figure 6). Firmware was created using guidelines found in the NDEF specification to access and write a message to the tag's SRAM. After the presence of an RF field is established, the RF430CL330H was waiting to be read or written by an NFC handheld device. In our case, an NFC enabled smartphone running an NFC tag reader application acted as our host.

The host was presented to the target board's antenna and the NDEF message was transmitted via RF link and displayed on the tag reader application screen. Then the tag reader application was used to change the NDEF message and write the new message back to the target board's memory.

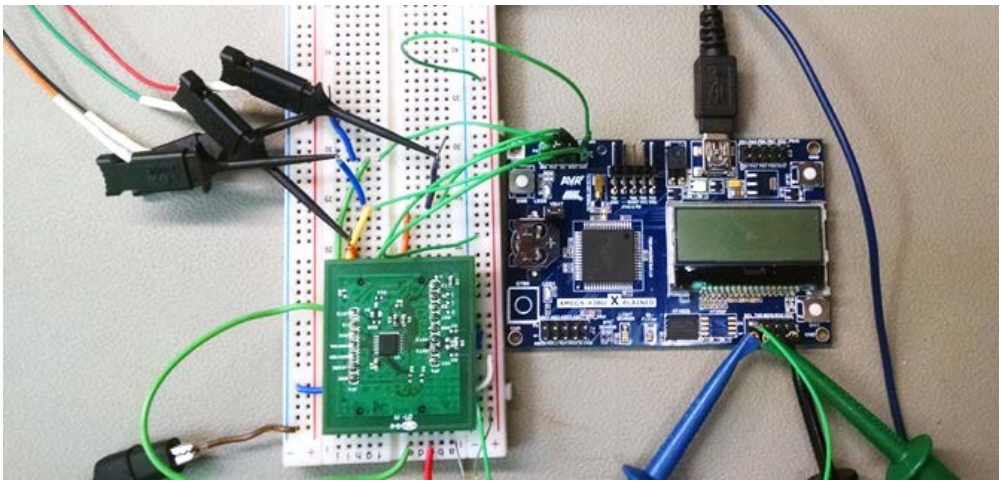

Figure 6. Breadboard Testing of NFC Data Transfer

While the ability to access the chips internal SRAM is critical, the memory capacity is much too small to be used as the primary means of data storage. Including ID and NDEF headers, the 3Kbyte NFC tag memory will allow for approximately 125 entries assuming a data frame structure made up of a 24 byte array. Augmentation to the internal memory was required so additional memory capacity for archiving historical measurements to non-volatile memory was applied in the form of the standard digital (SD) memory card format. The onboard SD card provides added security in the unlikely event of battery depletion; previously stored data will not be lost. The data capacity of the SD card is so large that more than 100 million data frame events could be stored, so it is unimaginable that the system would run out of storage memory. With the variety and flexibility of card capacities, the device memory can be increased by many orders of magnitude and allow for manual recovery and removal of data if desired.

To take full advantage of the added storage capacity, communication between the SD card and the RF430CL330H SRAM was necessary. Figure 7 illustrates the full system transmission of data from sensor to user.

When a train is detected, the MCU wakes to activate the sensors. After the absence of a train is acknowledged, an event data frame is created by the MCU and stored to the SD card. This process continues until the user wishes to extract the information that has been recorded. When the device detects the RF presence of a host requesting data, a read command is sent to the MCU. The MCU pulls the stored data from the SD card and writes it to the RF430CL330H SRAM in the form of an NDEF message. Finally, the data is extracted to the host reader where it can be viewed and stored.

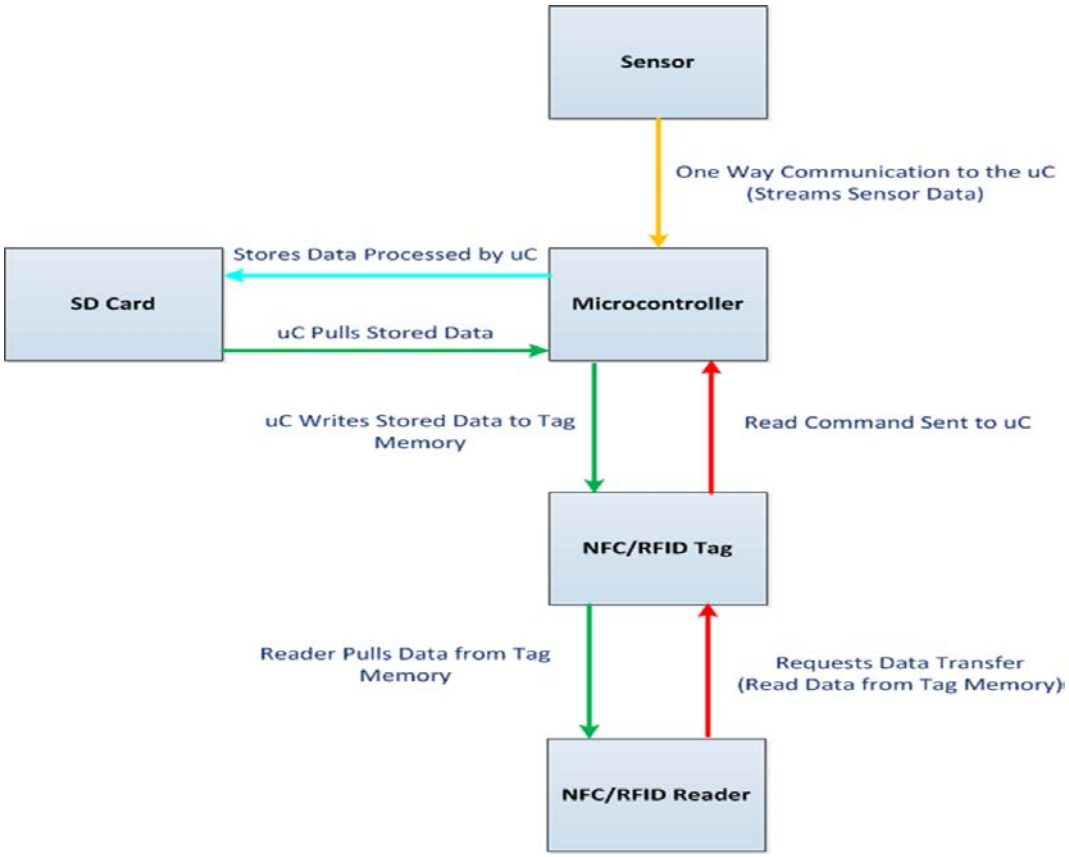

Figure 7. System Data Transmission Flow

A frame format comprised of a Device Identification Header and an Event Data Frame Structure is generated, which allowing events to be separately addressed after extraction. Table 1 depicts the frame structure. It was proposed that each device will have an Identification Header classifying essential information related to device location, firmware, memory size, and installation date. The Event Data Frame produced with each train pass will outline key information related to that event. The frame structure will include information such as event start time, total loaded and unloaded wheels and an event stop time.

Table 1. Event Data Frame Format

Identification Header
DESCRIPTION
Unit model identifier
Unit serial number
Sensor ID number
Firmware version number
Memory size
Installation location identifier
Installation location GPS - Lat
Installation location GPS - Lon
Installation date (month, day , year)
Installation time (hour, minute, second)
Rail line identifier
Installing Agency
Installation technician
New installation / re-installation

Event Data Frame Structure	
BYTE #	DESCRIPTION
Byte 0	Start Byte
Byte 1	Start of Frame
Byte 2	Data Frame Count (0 to 255)
Bytes 3, 4	Sensor ID number (MSB, LSB)
Bytes 5, 6	Event Number (MSB, LSB)
Bytes 7, 8, 9	Event Start Date Stamp (DD, MM, YY)
Bytes 10, 11, 12	Event Start Time Stamp (hh, mm, ss)
Bytes 13, 14	Total Loaded Wheels – this event (MSB, LSB)
Bytes 15, 16	Total UnLoaded Wheels – this event (MSB, LSB)
Bytes 17, 18, 19	Event Stop Time Stamp (hh, mm, ss)
Byte 20	Reserved
Byte 21	Reserved
Byte 22	End of Frame
Byte 23	End Byte

3.2 Lab Testing & Results

Prior to initial field testing, the developed data collection system was evaluated under controlled conditions. This testing was important, not only for operational verification of the accelerometer-based system, but as a method for providing comparisons to known stimuli. As shown in Figure 8 and Figure 9, the team's lab-based test setup employed a vibration generating mechanical shaker to provide excitation for side-by-side evaluation of a known geophone sensor and the digital sensors.

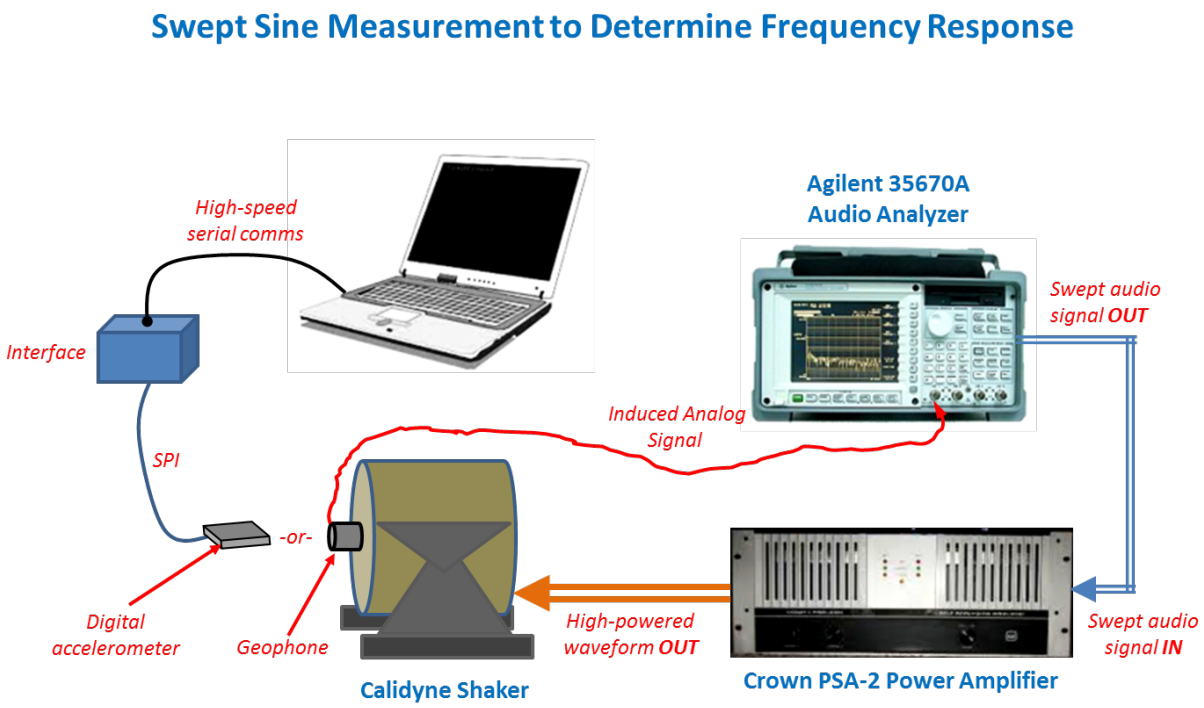

Figure 8. Controlled Signal Collection Configuration

Figure 9. Bench Test Setup

Digital accelerometers are very complex devices that include a micro-machined analog sensing element, anti-aliasing filtering, and a gain stage; then the component digitizes and encodes the results into an outgoing digital data stream. The chip-based sensor has numerous programmable options, and when questionable results were generated in the beginning of the program, the test setup proved invaluable in generating "ground truth" excitations for measurement evaluations. However, after fully investigating acceleration sensors and the various methods of processing data, the decision was made to evaluate non-acceleration-based sensors as well.

3.3 Field Testing & Results

After the initial design phase and lab testing of the acceleration sensor system was completed, field tests were performed on the New Hope Ivyland Railroad tracks during low-speed freight movements. Testing expanded to include SEPTA rail lines, with higher speed freight rail and commuter train movements. The inclusion of ultrasonic sensors in later tests is addressed in Section 4. Included below is an outline of field testing, including specific test parameters and metrics.

<u>New Hope Ivyland Rail Test #1 – 19 AUG 2014</u>

a) Two accelerometer units mounted approx. 6" away from each other and 4.5" down the web
b) Mount comprised of magnetic attachment with rubber damping strips
c) Recorded data using HyperTerminal program (3200Hz sampling rate)
d) Started the test using a hammer to hit the rail and record measurements at 10' intervals along the track
e) Train and loaded cars traveled back and forth multiple times (number of cars per event not recorded)
f) Visually observed large amount of rail deflection
g) After monthly meeting, it was decided that the team needed a way to visualize and record incoming data from sensors in real time (GUI, ability to "tag" wheel crossings)

<u>New Hope Ivyland Rail Test #2 – 05 SEP 2014</u>

a) Two accelerometer units mounted approx. 7" away from each other and 4.5" down the web
b) Mount comprised of magnetic attachment with rubber damping strips
c) Observed several train movements, recorded real-time data with GUI (3200Hz sampling rate)
d) Train movements on secondary side rail as well as primary rail with sensors mounted
e) Data displayed during test did not make sense and the team discovered a problem with data transfer speed within the collection software.
f) All data determined contaminated
g) Identified the need to determine "ground truth" data measurements

<u>New Hope Ivyland Rail Test #3 – 12 SEP 2014</u>

a) Measured several train movements using the dual accelerometer setup from NHIR Test #2; the real-time data was recorded with a PC-based GUI (3200Hz sampling rate)
b) Sensor mounting comprised of magnetic attachment with rubber damping strips

c) A remote computer time based display (monitor and BigClock program) was added for event synchronization. The BigClock was in the field of view for the recorded video and directly linked to the PC data file header information
d) To take simultaneous measurements of the train movements, a spectrum analyzer and geophone (our "ground truth") was added in this test.
e) Results determined that a better synchronization method provided more exacting wheel positioning with the recorded acceleration data than the BigClock display.

New Hope Ivyland Rail Test #4 – 19 SEP 2014

a) Observed several train movements, recorded real-time data with GUI (3200Hz sampling rate) using the dual accelerometer setup from NHIR Test #2
b) Mount comprised of magnetic attachment with rubber damping strips
c) Same test setup as NHIR test #3, with the addition of an ultrasonic range finder installed between the two accelerometers sampled simultaneously with the accelerometers
d) Identified need to determine best sampling rate

Crestmont Station SEPTA Line - Test #1 – 26 SEP 2014

a) Test setup includes magnetic attachment with rubber damping strips
b) Two accelerometers with one ultrasonic range finder centered between the sensors
c) Display of PC internal clock time and video camera to capture events
d) Two sampling rates tested (400Hz, and 1600Hz)

First Event: 12:25:00 AM

- Engine, five freight cars, engine
- Speed approximately 20-25 mph (northbound)
- Train slows then speeds up again (verified in ultrasonic data)

Second Event: 01:20:00 AM

- Single SEPTA passenger car
- Seed approximately 40 mph (northbound)

Third Event: 01:30:00 AM

- Engine, single freight car, engine (return of equipment from event 1)
- Speed approximately 25-30 mph (data shows noticeable clipping?)

Crestmont Station SEPTA Line - Test #2 – 16 OCT 2014

a) Dual data collection systems (4 total accelerometers)
b) Testing of decoupling materials on sensor attachments (rubber feet vs. foam tape)
c) Display of PC internal clock time and video camera to capture events
d) Two sampling rates tested (100Hz and 1600Hz)
e) Test setup includes 4 accelerometers and Ultrasonic Sensor
    - Decoupled using foam tape @ 100Hz sampling rate
    - Decoupled using foam tape @ 1600Hz sampling rate
    - Ultrasonic sensor
    - Decoupled using rubber feet @ 100Hz sampling rate
    - Decoupled using rubber feet @ 1600Hz sampling rate

First Event: 12:25:00 AM

- Engine, two tank cars, one box car, one tank car, engine
- Speed approximately 20-25 mph (northbound)

Second Event: 12:40:00 AM

- Three SEPTA passenger cars
- Train stopped at Crestmont station to discharge passenger (northbound)

Third Event: 01:30:00 AM

- Two engines (return of equipment from event#1)
- Speed approximately 25 mph (southbound)

Crestmont Station SEPTA Line - Test #3 – 04 DEC 2014

a) Dual data collection systems (4 total accelerometers)
b) Display of PC internal clock time and video camera to capture events
c) Testing of higher-input rated accelerometer (±200g) and ultrasonic sensor
   - One ±200g accelerometer (3200 Hz sampling rate)
   - Ultrasonic sensor
   - One ±200g accelerometer (3200 Hz sampling rate)
   - One ±16g (1600Hz) accelerometer mounted mid-rail web as a reference
   - One ±16g (1600Hz) accelerometer mounted on rail-tie plate (deflection)
d) New sensor mounting techniques used
   - ±200g sensor hard clamped to rail (screw fastened to one piece aluminum mounting fixture)
   - ±16g sensors magnetically mounted, decoupled with rubber feet

First Event: 12:30:00 AM

- Engine, six tank cars, one box car, an engine
- Speed approximately 20-25 mph (Northbound)

Second Event: 12:43:00 AM

- Three SEPTA passenger cars
- Train stopped at Crestmont station to discharge passenger (Northbound)

Third Event: 01:42:00 AM

- Engine, three tank cars, an engine (return of equipment from event #1)
- Speed approximately 25 mph

Bethlehem Industrial Branch - Test #1 – 29 DEC 2014

a) Dual data collection systems (4 total accelerometers)
b) Displacement and phase testing
c) Mounting configuration
   - Two ±200g accelerometers screw fastened to beam clamp, attached to rail flange (inner sides of adjacent ties) - phase measurements (3200Hz sampling rate)
   - Ultrasonic sensor between ±200g sensors
   - ±16g sensors magnetically mounted to tie plates of opposite rail, decoupled with foam tape - displacement measurements (1600Hz sampling rate)

First Event: 15:31:00 PM

- Three cars pushed by one engine

- Speed approximately 15 mph (Northbound)

Second Event: 15:41:00 PM

- Engine pulling fifteen cars
- Speed approximately 15 mph (Southbound)

Third Event: 15:45:00 PM

- Fifteen cars being pushed by engine (return of equipment from event #2)
- Speed approximately 15 mph (northbound)

The dynamic interaction between the train and the supporting rail generated a complex signal that was impossible to recreate in the lab environment. Extensive field testing allowed the data to be collected through controlled placement and condition of the implemented sensors. The ultimate goals were to count the train wheel passages and simultaneously obtain a relative estimation of weight as the wheel transitioned by the sensor(s). It was hoped that a pair of accelerometers could be used to accomplish these goals by comparing similar and dissimilar signals.

The team explored numerous test conditions beyond the previously mentioned mechanical coupling and attachment issues. Sensor sampling rates and measurement input ranges were varied as the team searched for a "simple" processing solution. The electrical power constraints limited the functionality available to our class of embedded processor analysis of the measured data. Even a low-end desktop PC offers a significant increase in computing "horsepower" in comparison to the microcontroller used in the TAG system. The time available to analyze the streaming data to record positional and weight estimates was also limited, because the analysis needed to be completed before the interaction of the next adjacent wheel. Opposing this was the power required to operate the MCU. Increased operating speed allowed more computational cycles per second but is proportional to the amount of power used.

Initially, only raw data from the sensors was recorded and various processing routines would be run during post-test analysis in the lab. Simple algorithms, like time domain addition and subtraction, were tried first in the effort to minimize power consumption. This extended to individual sensor inter-axis examination and continued to include the data simultaneously collected by the neighboring accelerometer. More complex techniques followed and included digital filtering, Fourier analysis and coherence measurements. Double integration of the acceleration data to yield positional information was explored and the complex, computationally-intensive single value decomposition processing was also employed. Illustrated in Table 2 is a concise overview of the processing efforts. An abridged representation of the analysis can be found in plotted data in an Appendix.[1]

[1] A large amount of data was collected at field tests on the New Hope Ivyland Rail, Crestmont Station SEPTA Line, and Bethlehem Industrial Branch. The full Appendix document includes over 400 pages of processed data and charts and is not included here due to length. Contact Navmar-AAS for a copy.

Table 2. Signal Processing and Analysis Methods

Sample of Signal Processing and Analysis Methods

- Analyze Single Sensor Axis and Across Sensor Axis (where applicable)
- Various sampling rates, filter frequencies and coupling materials

	X-Axis	Y-Axis	Z-Axis
FFT Analysis	√	√	√
Low Pass Filter	√	√	√
Band Pass Filter	√	√	√
Double Integration (displacement)	√	√	√
Cross-correlation Between Axis	X vs Y	Y vs Z	Z vs X
Axis Addition	X+Y	Y+Z	Z+X
Axis Subtraction	X-Y X-Z	Y-X Y-Z	Z-X Z-Y
Moving Average	√	√	√

	X-Axis	Y-Axis	Z-Axis
Dual Sensor Axis Subtraction (amplitude phase)	$X^1 - X^2$	$Y^1 - Y^2$	$Z^1 - Z^2$
Dual Sensor Double Integration (displacement phase)	$X^1 - X^2$	$Y^1 - Y^2$	$Z^1 - Z^2$
Single Value Decomposition	√	√	√
Various Sensor Sampling Rates	√	√	√
Various Sensor Coupling Materials	√	√	√
Various Sensor Mounting Methods	X+Y	Y+Z	Z+X

3.4 Conclusions

The limited processing capability available within the TAG unit was incapable of consistently differentiating individual train wheel sets from the numerous data measurements of vibrational energy captured through the ADXL345 and ADXL375 accelerometers. In some cases, determining deflection by way of double integration of the accelerometer data, in conjunction with acceleration data of high energy wheel passes, showed promise in isolating points of interest but, as shown in Figure 10, this processing was not sustainable across multiple test locations and scenarios. Also, exploiting these points of interest would require intensive computational processing, and these CPU intensive algorithms would prove inadequate for this design based on the time available between wheel cycles for event processing.

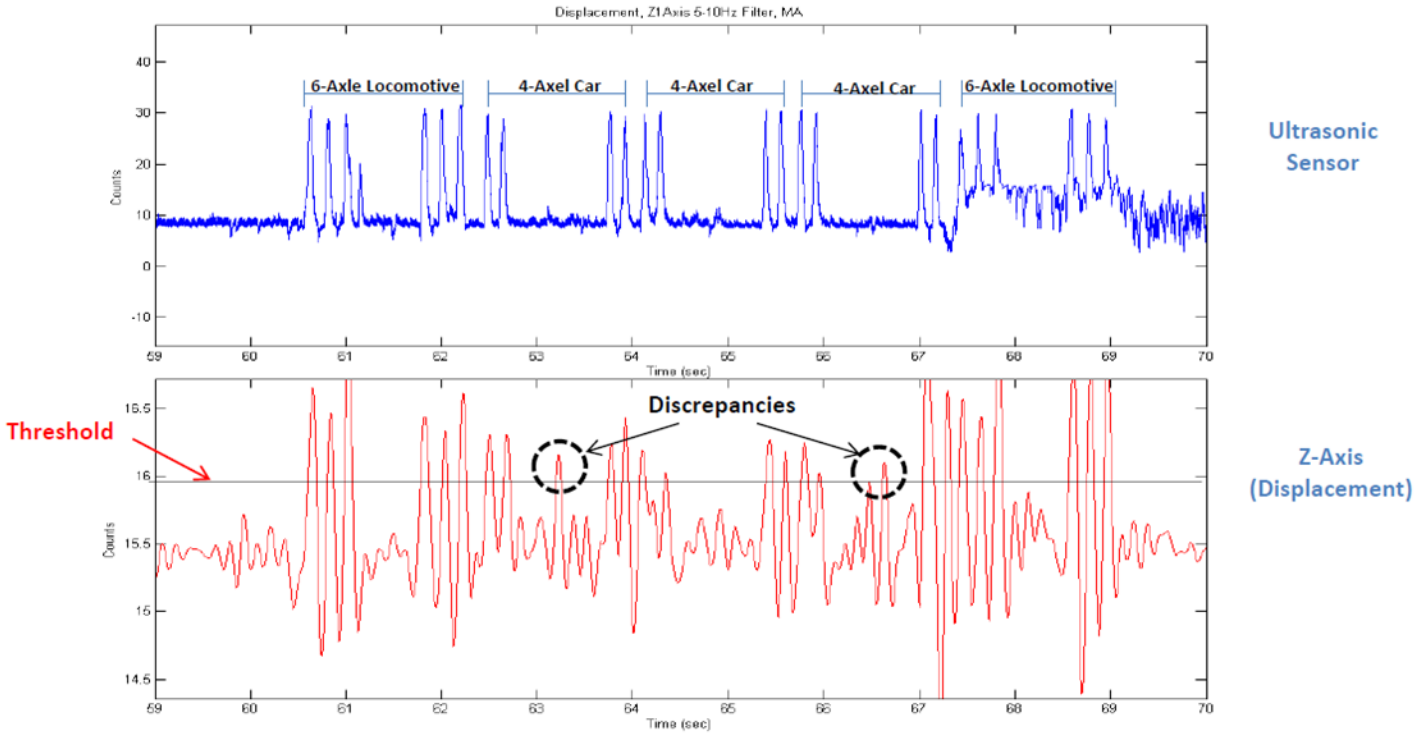

Figure 10. Accelerometer Deflection Results – Crestmont SEPTA Test #3

The accelerometer sensors were successful in demonstrating the ability to distinguish relative loading events and they were leveraged to provide estimations of loaded versus unloaded by using the initial train engine measurements as a gauge for the assessments (Figure 11). This relative comparison allows for inconsistencies in mechanical and geophysical placement locations and is a more realistic approach than attempting to implement a rigid, static parameter that designates loaded or unloaded rolling stock. In addition, the load determination can be accomplished by use of a single accelerometer, as the principle measurement is based on received energy signatures and not a comparison between a pair of sensors. The use of a single acceleration sensor helps to reduce power consumption, complexity and cost.

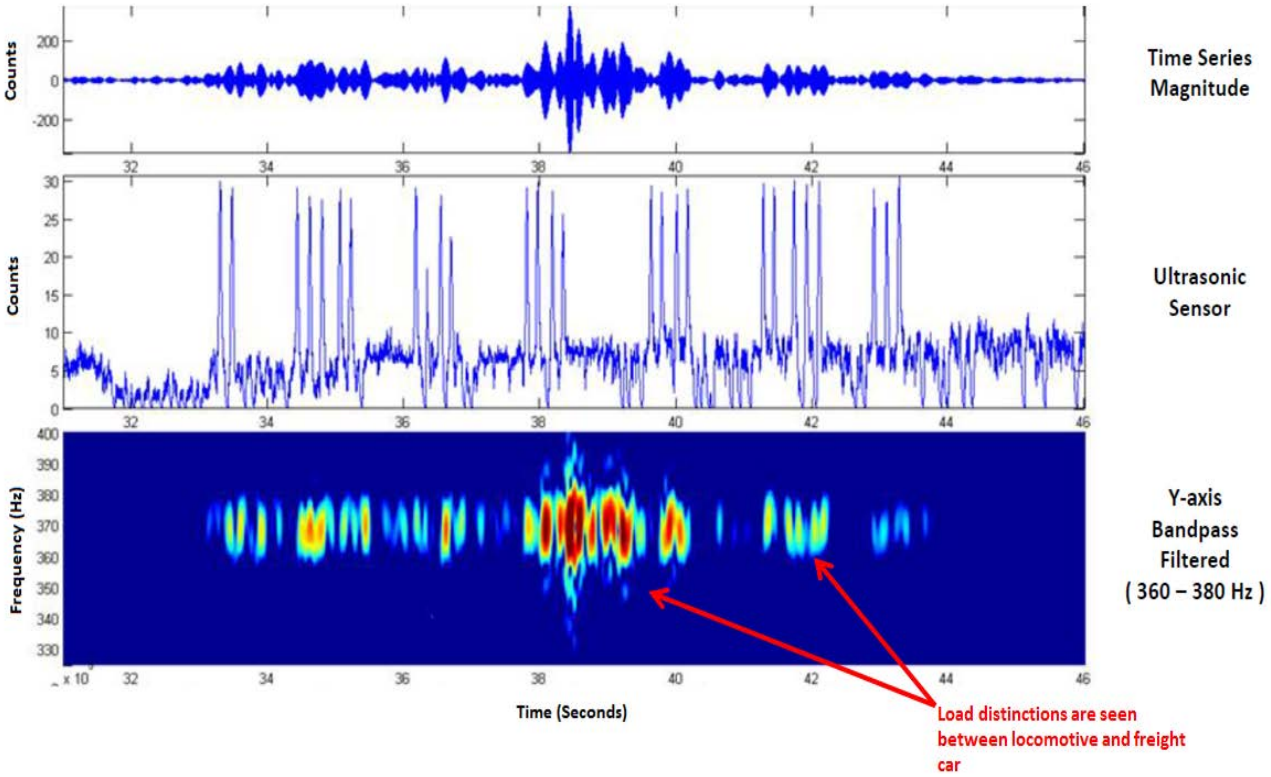

Figure 11. Load Distinction Using Single Accelerometer – Crestmont SEPTA Test #3

4. Final System Development

4.1 Sensor System Development

The original approach to this research project's design was to use a pair of acceleration sensors to both determine the exact time and count of train wheel passages and to provide a relativistic prediction of the status of each passing wheel set as being loaded or unloaded. Test results revealed that a single acceleration sensor could provide adequate sensor information to make a reasonable prediction of the relative loading of passing wheel sets. However, within our constraints of cost, power usage, size and unrestricted installation locations, the pair of acceleration sensors and associated processing, did not to accurately and consistently determine wheel passage events.

During testing, the HMC5883L magnetometer demonstrated a high degree of accuracy in sensing the train wheels and is considered to be a viable sensor for this team's goals. This sensor requires minimal power while operating, so is well suited for a battery-powered system. In lieu of a pair of accelerometers, a low power HMC5883L tri-axial magnetometer demonstrated a much greater ability to identify individual wheel events when used as a ferrous material detector. When a train wheel was in the proximity of the sensor, large variations in the local magnetic field were indicated on all three axes. These variations were used to detect wheel sets using a straightforward processing method to establish a threshold level. Once a threshold is identified, incremental wheel counts can be attained when measured magnetic data exceed that level.

Figure 12 and Figure 13 compare the performances of the ultrasonic rangefinder module and the magnetometer during field testing. The ultrasonic was the exacting reference used throughout the series of acceleration field testing. It performed well but was not a practical solution for the TAG due to unit cost, sensor positioning requirements, and the unrealistic power consumption requirements for a battery-based system. The magnetometer provides similar results at a fraction of the cost and with several orders of magnitude reduction in system power requirements.

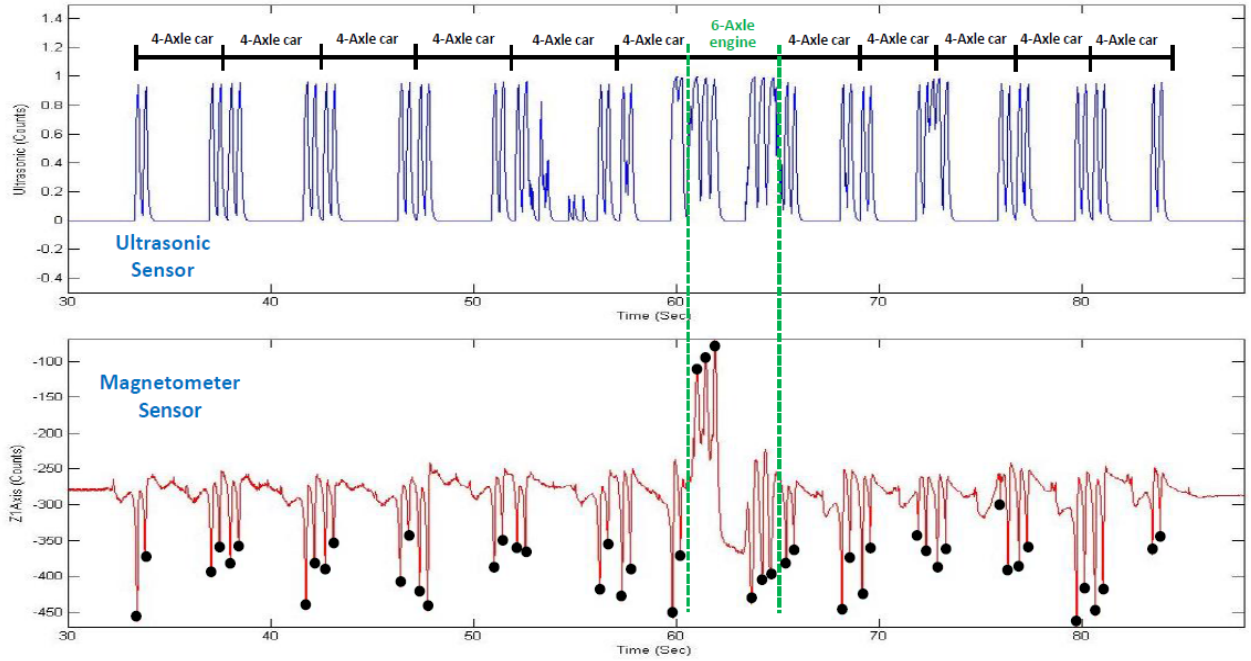

Figure 12. Magnetometer Wheel Distinction – Bethlehem Branch Test #3

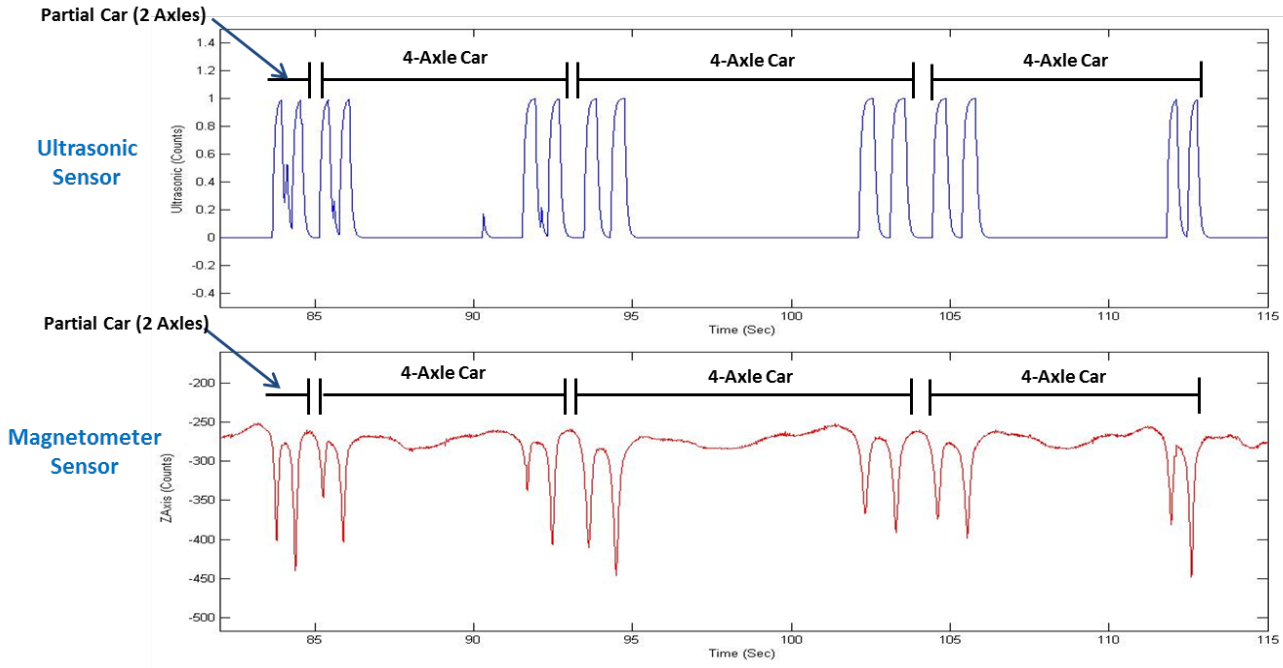

Figure 13. PNRR rail results – detection of train wheel comparison between magnetic field sensor and active ultrasonic rangefinder unit

4.2 Lab Testing & Results

Navmar examined a wide variety of magnetic and ultra-sonic based devices (see Figure 14) based on a set of acceptance criteria that included functionality, size, power requirements, and cost. The magnetism-based devices based on Hall Effect, magnetic proximity, and magnetometers performing as ferrous metal detectors were assessed on their ability to sense changes in magnetic fields. The ultrasonic proximity sensors employed a single or dual pair of transducers to output a burst of sound and calculate distance to an object based on the time taken to receive the return wave.

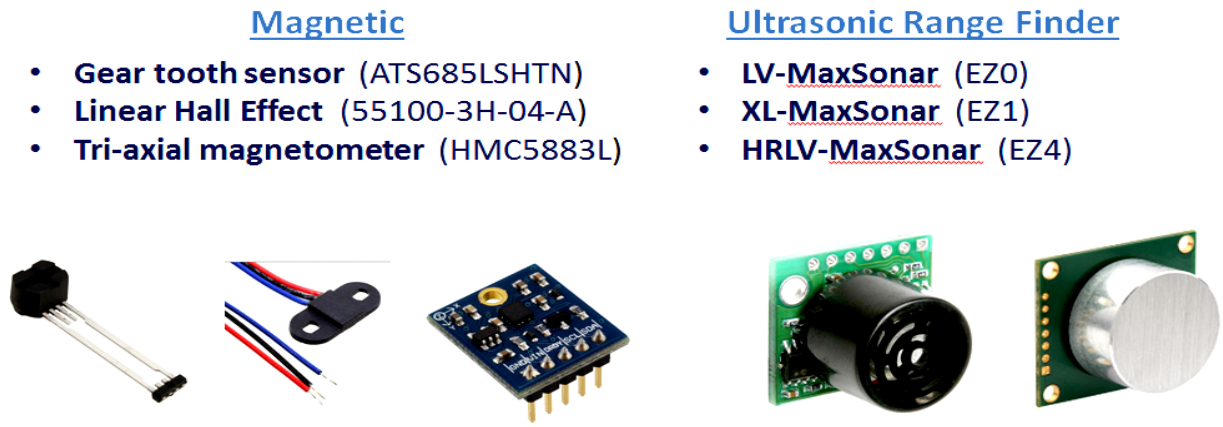

Figure 14. Non-Vibration-Based Devices

These sensors were tested in the lab using a 28-inch diameter, flanged wheel from the Philadelphia Electric Trolley Museum and a 3' segment of rail. Navmar conducted controlled tests, recorded data, and evaluated each senor. To reduce fixture complexity and increase safety, the wheel was placed in a stationary, horizontal position and tests were performed by traversing a rail segment that was horizontally adjacent to the wheel (Figure 15).

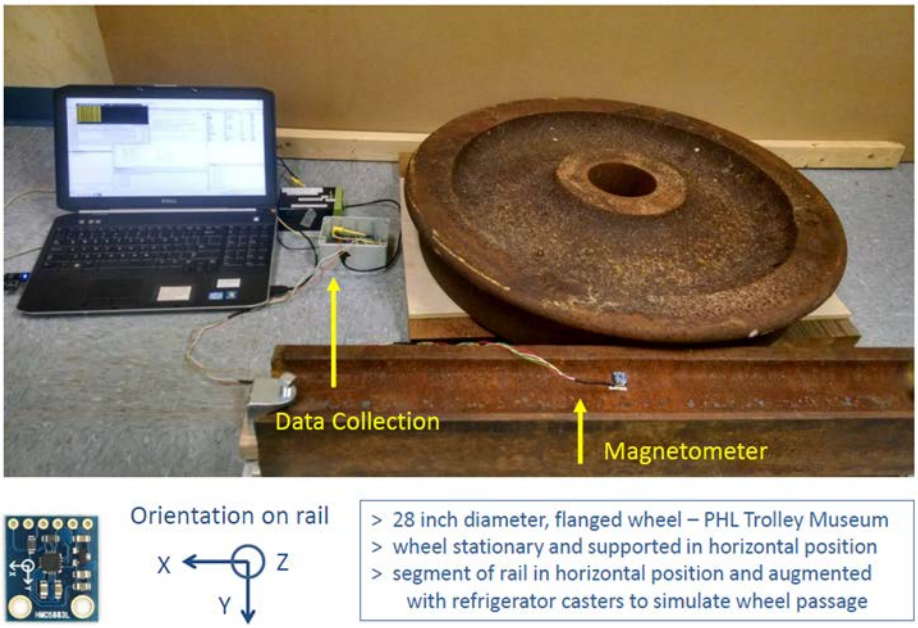

Figure 15. Lab Setup - 28" Diameter Wheel and Rail Segment

The device senses the presence or absence of a train wheel and it must be paired with an accelerometer or other device for weight determination. Table 3 provides details and additional information from the sensor evaluation process.

Table 3. Sensor Comparison and Evaluation

Sensor	Pros	Cons
Magnetometer (HMC5883L)	• Discrete form factor • 0.1mA supply current • Wide magnetic range sensitivity • Lab testing shows promise	• Yet to determine if large mass of metal from train will alter results
Gear Tooth (Proximity) (ATS685LSHTN)	• Discrete form factor • 6mA supply current • Can be packaged for environment	• Air gap range too tight • Impossible to mount close enough for sensing
Linear Hall Effect (55100-3H-04-A)	• Larger operational air gap • 5.2mA supply current • Environmentally protected	• Wheel required to block magnetic field to operate • Proper sensor mounting is challenging
Ultrasonic XL (MaxSonar-EZ1)	• Easy to use interface • 2.5 cm resolution • 2 mA supply current • Various calibrated beam widths	• Larger form factor • Environmental version $100 • Low sampling rate
Ultrasonic HRLV (MaxSonar-EZ4)	• 1 cm resolution • 2 mA supply current • Various calibrated beam widths • Real-time noise rejection	• Larger form factor • Environmental version $100 • Low sampling rate

The HMC5883L magnetometer was the top candidate for further testing. Magnetic-based sensors require impractical air gap and mounting conditions. The ultrasonic proximity devices showed promise but environmentally packaged versions of the sensors are costly, and proper placement and alignment of the field of view is critical to performance.

Navmar conducted additional tests of the HMC5883L sensor to determine mounting location and orientation sensitivity with respect to the mass of ferrous material from the train. Various mounting locations along the rail web were tested.

The following plots contain measured results from moving the rail segment alongside the train wheel, back and forth, for a total of 10 passes. The first set, shown in Figure 16, examined the sensor in the vertical orientation where the Z-axis was the expected dominant. The image shows measurements recorded with the HMC5883L mounted closest to the top of the rail vs. farthest away. The rapid signal decrease indicates wheel passage. Promising results were captured in both cases, however, the difference between wheel presence versus wheel absence was larger when the sensor was mounted closest to the top of the rail.

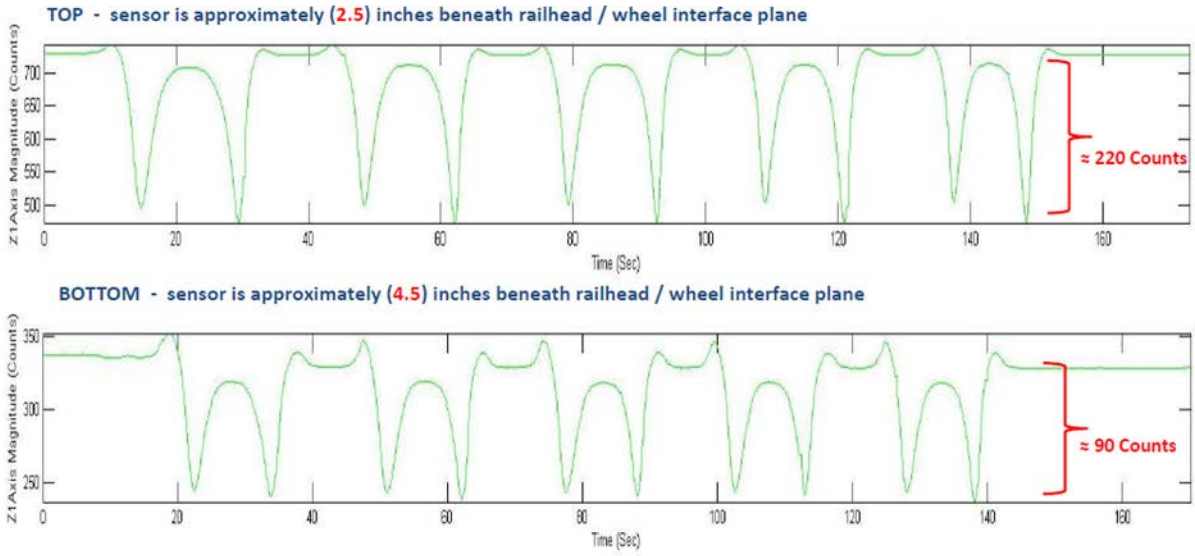

Figure 16. Lab Test Results – Vertical Positioning Sensitivity

Figure 17 shows plots where the HMC5883L was rotated 90 degrees in the horizontal position. These plots illustrate a difference in amplitude magnitude with the dominant axis being the X-axis. The amplitude ranges measured are comparable to the vertical sensor orientation, again showing increased sensitivity when mounted closer to the top of the rail.

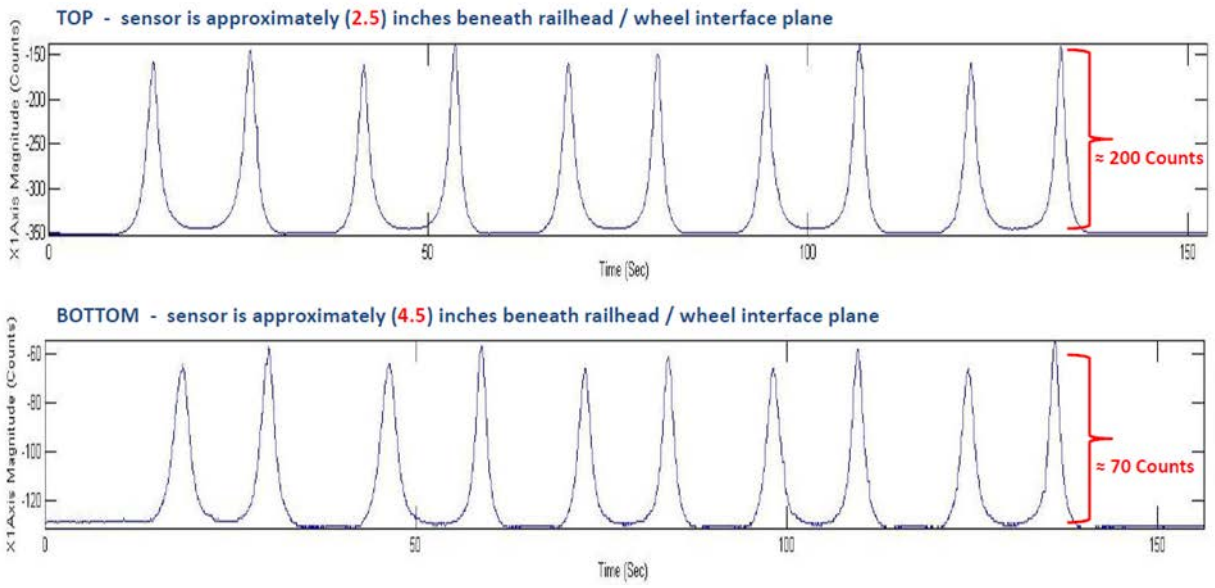

Figure 17. Lab Test Results – Horizontal Positioning Sensitivity

Finally, the data plots in Figure 18 illustrate the difference between mounting the magnetometers on the inside, or outside of the rail web at the same vertical height closest to the top of the rail. The inside position takes advantage of the inner flange of the train wheel, especially in the Z-Axis. The results from these tests conclude that the ideal placement of the HMC5883L is in the vertical orientation, on the inside of the rail, closest to the top of the web.

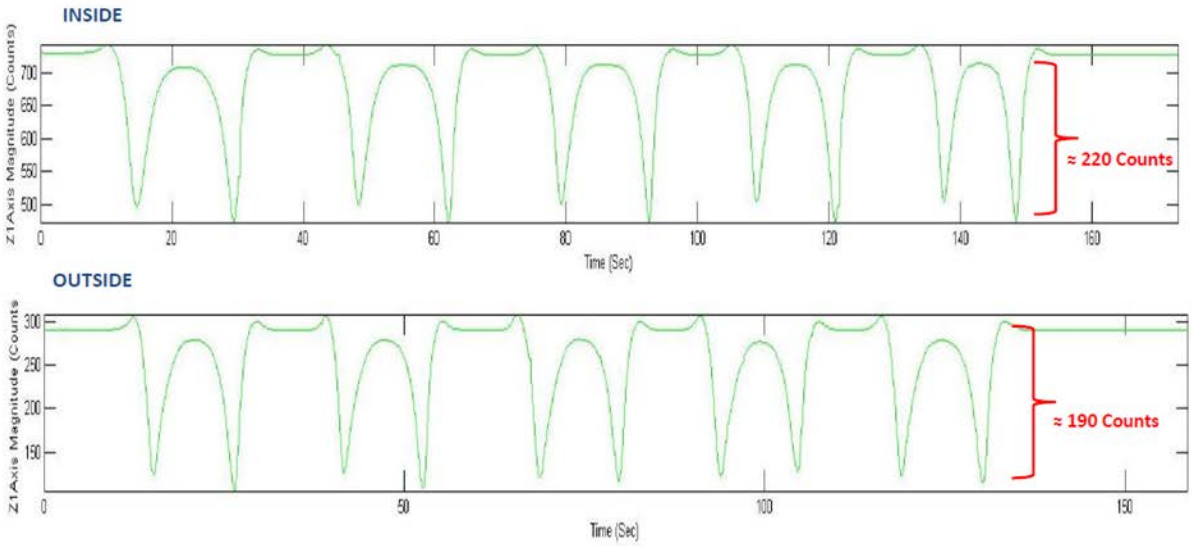

Figure 18. Lab Test Results – Web-Face Positioning Sensitivity

4.3 Field Testing & Results

After field testing, the system was evaluated along the Bethlehem Industrial Branch near Lansdale, PA. Below is an outline of tests, including parameters and metrics.

Bethlehem Industrial Branch - Test #2 – 09 MAR 2015

a) Non-vibrational test (no accelerometers)
b) Demonstrate magnetometer operation in presence of train
c) Test low power ultrasonic sensor
d) Test setup
    - Two magnetometers mounted to inside of track web (15Hz sampling rate)
    - Magnetometers mounted via hard clamp attachment
    - One magnetometer in horizontal orientation, one in vertical orientation
    - MaxSonar low power ultrasonic sensor mounted next to magnetometer pair
    - Original Parallax ultrasonic sensor, mounted on outside of track between magnetometer pair

First Event:

- Engine pulling eight cars
- Speed approximately 15 mph (northbound)

Second Event:

- Engine pushing 5 empty cars
- Speed approximately 15 mph (southbound)

Third Event:

- Engine pulling 5 empty cars
- Speed approximately 15 mph (northbound)

Bethlehem Industrial Branch Test #3 – 17 MAR 2015 (Re-test of Bethlehem Test #2)

a) Increased sampling rate (75Hz) for better resolution to resolve issue of missed wheels identified in previous test, presumed to be a result of low sampling rate
b) Operated only one ultrasonic sensor at a time, switching between the Parallax and the MaxSonar, to eliminate ultrasonic sensor interference noticed in previous test
c) Graphical display was updated for monitoring real-time data collection of magnetometer and ultrasonic measurements

First Event:

- Five cars, engine, six cars
- Speed approximately 15 mph (southbound)
- Active ultrasonic sensor - Parallax

Second event:

- Six cars, engine, five cars
- Speed approximately 15 mph (northbound)
- Active ultrasonic sensor – Parallax

Third event:

- Five cars, engine, five cars
- Speed approximately 15 mph (southbound)
- Active ultrasonic sensor – MaxSonar

4.4 System Power

The team defined an improbable freight traffic density over a typical month so they could estimate the battery's lifetime. When this estimate was calculated, it was assumed that fifteen freight trains, with each train consisting of 4 locomotives and 100 freight cars, would pass the TAG sensor per day at an average speed of 35 mph. This results in a total of 450 trains, or 46,800 pieces of rolling stock, in a one month period. Considering an average car length of 67 ft. and the known system power requirements, a representative active duty cycle could be determined and used to predict the total monthly current consumption. With the predicted current consumption, available battery chemistries were evaluated to verify if reasonable sensor operating life was possible.

A variety of battery types were considered, but ultimately two C-size Lithium-Thionyl Chloride (LiSOCL2) batteries in parallel were chosen as a suitable option that met both size and power density requirements. Using the above specified operating conditions, and the advertised capacity of existing batteries, it was determined that a Tadiran TL-2200 C battery would provide sufficient power for TAG to operate under the specified conditions for close to seven years (Figure 19).

# Cars	# Locomotives	Car Length (ft)	Total Train Length (ft)	# Wheels / rail	Speed (mph)	# Trains / Month
100	4	67	6968	424	35	450

Battery	Cell Size	Chemistry	Discharge Voltage	Capacity (mAh) @ .2mA Continuous draw @25 deg C	Battery life (Months)	Battery Life (Years)
Tadiran TL-2200	Two C cells in parallel	LiSOCl2	3.6	13200	81.98	6.83

Feet / Mile	5280
Speed (feet/hour)	184800
Speed (feet/Minute)	3080
Speed (feet/Second)	51.33
Time for 1 train to pass (Sec)	135.74
Time for 1 train to pass (Min)	2.26
Time for 1 train to pass (Hrs)	0.038
Seonds in one month	2629400
Total Monthly Active time (Sec)	61083
Total Monthly Idle time (Sec)	2568317
Minutes in one month	43829
Total Monthly Active time	1018
Total Monthly Idle Time	42811
Hours in one month	730.49
Total Monthly Active time (Hrs)	16.97
Total Monthly Idle Time (Hrs)	713.52
Total Active Current (mA)	2.420
Total Idle Current (mA)	0.1681
T_active (seconds) / month	61083
T_idle (seconds) / month	2568317
Average Current (mA) 2.323% Duty Cycle	0.220

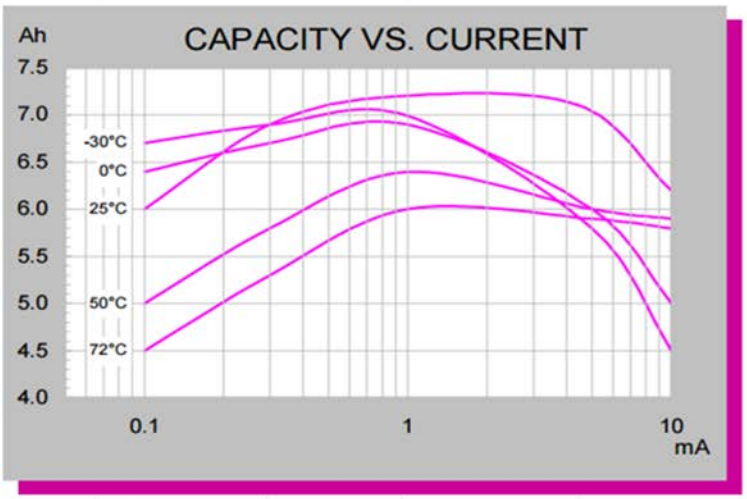

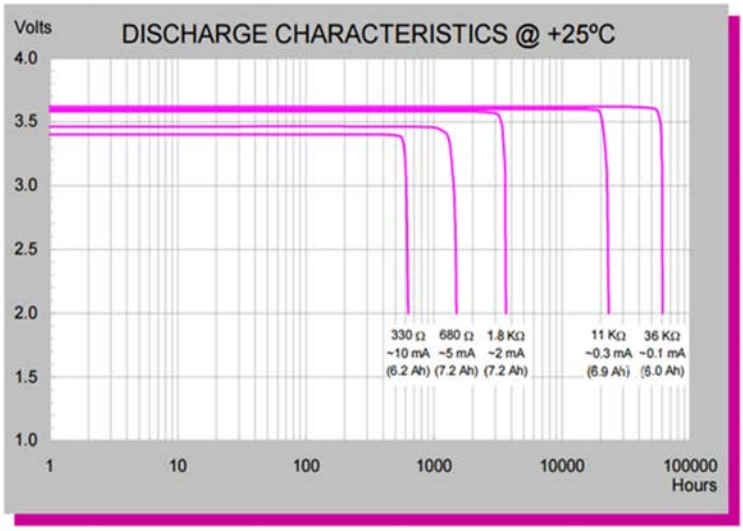

Figure 19. Battery Life – Freight Traffic Example

The high current capacities of standard Lithium batteries offer an optimal solution for powering low current devices over a long period of time. Lithium-Thionyl batteries like the TL-2200 have the highest energy density of any practical lithium chemistry, three times greater than alkaline batteries, and are widely used in commercial applications.

4.5 Enclosure Development

The TAG enclosure was designed for durability, which gives it the ability to resist the environment and any vandalism attempts. As snow and flooding along the track area are included among the potential hazards, the unit must have the ability to survive shallow depth immersion in water (NEMA 6/IP67 equivalent).

Figure 20 shows the circuit card assembly, RFID antenna, components and installed batteries. The circuit card is mechanically attached to the aluminum backing plate and allows the accelerometer, mounted on the rear side of the circuit card, to be in intimate contact with backing plate. The mounting plate also includes two integral female threaded studs that pass through holes in the circuit card, for attachment of the mounting bracket clamp.

Given the potential further development of the TAG, other packaging design concepts become candidates depending on operational requirements and production quantities. In sufficient quantities, encapsulation is a possibility that provides a very robust package at minimal cost. The downside is that the batteries must be permanently installed and the unit is useless once the batteries are expended. A study is necessary to determine if the estimated 5-year operational life is sufficiently long to justify the unit cost per day of service of an expendable device that is discarded after battery exhaustion. A potential encapsulated TAG concept is rendered in Figure 21.

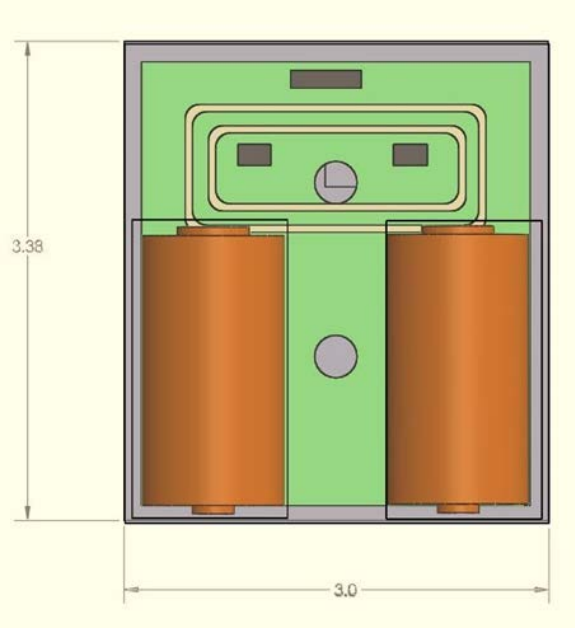

Figure 20. TAG System Packaging

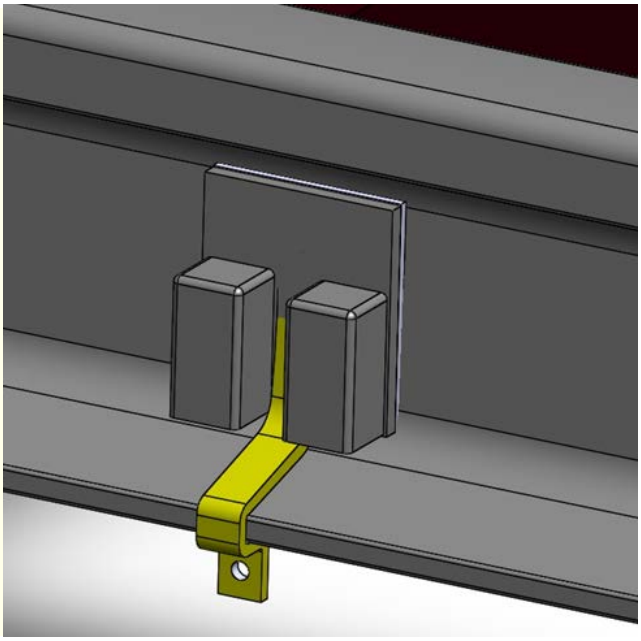

Figure 21. Encapsulated TAG Package

The second packaging approach is a two-piece unit that includes a gasketed cover. Once the unit is joined together, an environmental seal would be formed between the two assemblies that renders the unit waterproof. This scenario provides less protection against physical attack but it does promote unit longevity by allowing the replacement of the system batteries.

Figure 22 and Figure 23 show the TAG as a two-piece unit.

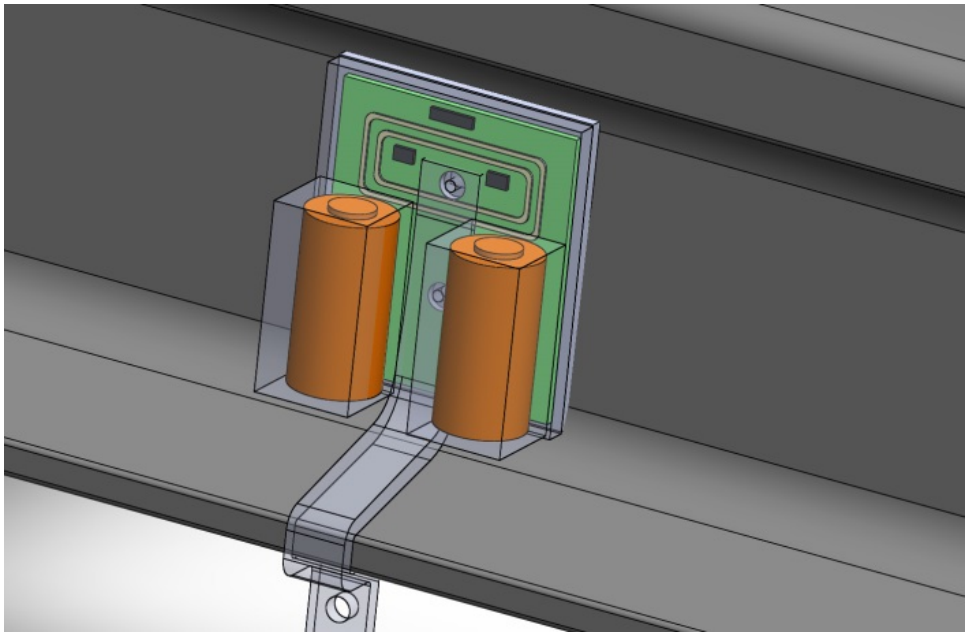

Figure 22. Two Piece TAG Unit on Rail

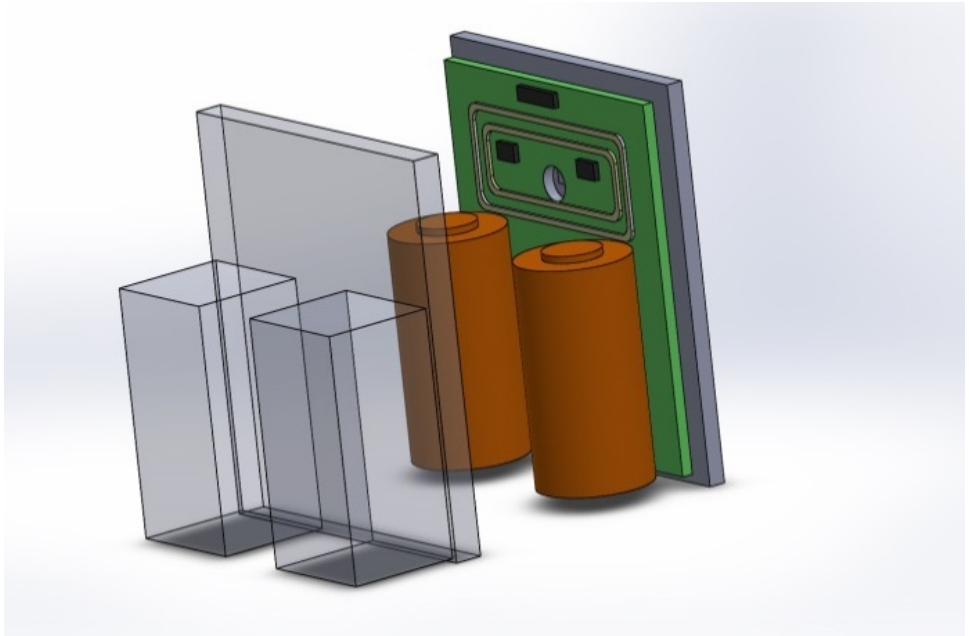

Figure 23. Exploded View of Two-piece TAG Concept

5. Conclusions

In Phase I of the FRA's *Wheel Load Cycle Tag for Rail* project, Navmar developed a sensor system to meet these requirements:

- Low cost
- Small form factor
- Environmental ruggedness
- Service life
- Energy harvesting potential (for system power augmentation)
- Easy rail installation
- Measurement accuracy
- Data transfer from rail device to handheld RF unit

To that end, we explored several sensors (acceleration-based, magnetic, and ultrasonic) and recommended a hybrid sensor system using an accelerometer for wheel load data and magnetometer for wheel count data. The individual parts of this system were tested in the laboratory and at field sites with great success. Though rigorous testing, we found that a single ADXL345/347 accelerometer sensor is capable of load determination, since the principle measurement is based on received energy signatures.

In addition, the low power HMC5883L tri-axial magnetometer demonstrated a much greater ability to identify individual wheel events. Using NFC technology, data can be transferred from the rail device to a handheld device. If a magnetometer is combined with an accelerometer to create a hybrid-sensor suite, they could achieve the defined objectives. The devices have been field-demonstrated individually, but they have not been demonstrated simultaneously in a combined system. Further development is required, but the risk of failure is low due to the successful operations that were previously conducted. Figure 24 provides a system overview as envisioned after reviewing the results of lab and field tests for all three sensors.

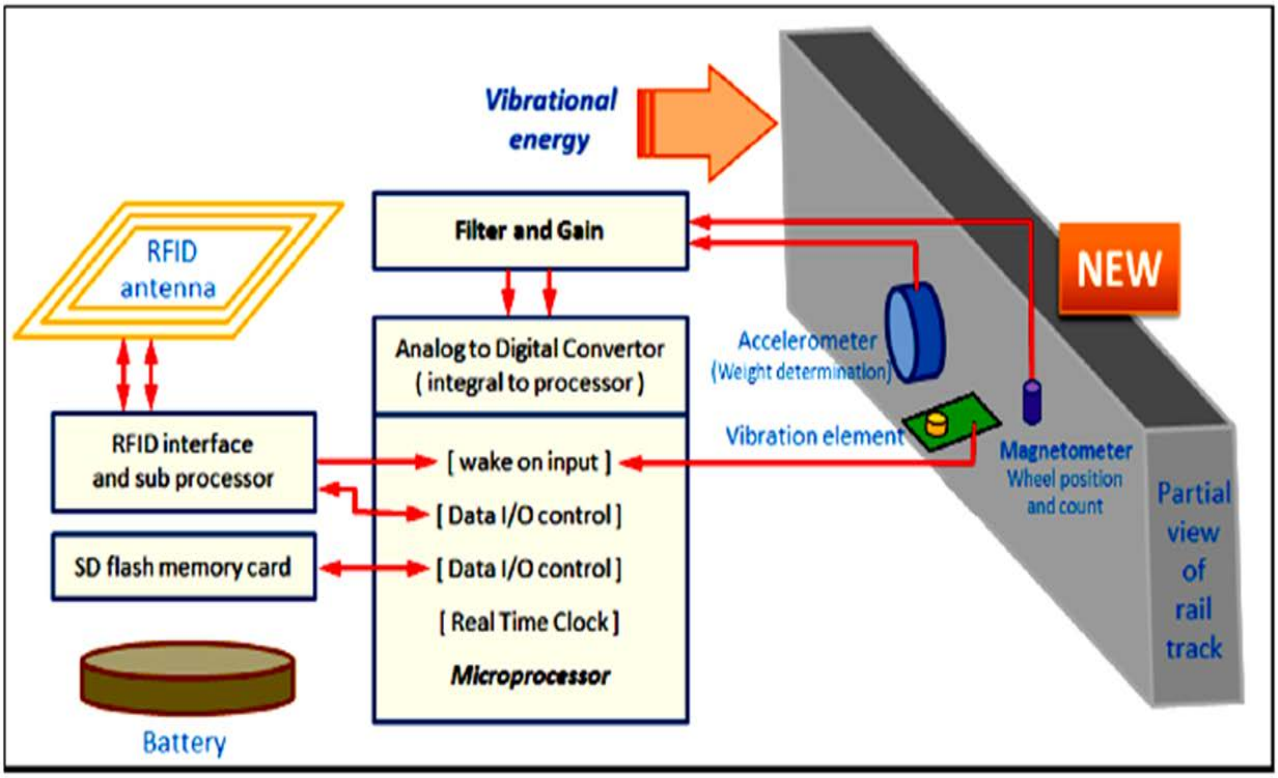

Figure 24. Overview of Rail Tag System

In terms of power, using standard operating conditions and the advertised capacity of existing batteries, it is estimated that a Tadiran TL-2200 C battery would provide sufficient power to allow the TAG to operate under the specified conditions for close to seven years. An enclosure concept has been developed and presented for further investigation, to meet the requirement of environmental ruggedness.

6. Recommendations for Continued Research

In rail safety, there is an urgent need to collect statistical usage data and ascertain the cumulative load-induced fatigue on rail track segments. The estimation of rail segment burdening by the determination of loaded or unloaded wheel passages, in conjunction with totalized counts, can provide statistics that serve as harbingers against track failure.

This research effort has great potential to solve this problem in an expeditious and cost-effective way. However, additional research is required to complete this task and offer a pre-production prototype design. Recommendations for future development work are listed below.

1. Conduct additional development and testing of a combined hybrid sensor suite to determine that the simultaneous wheel load classification accomplished using the ADXL375 can function in parallel with the operation of the magnetometer sensor. Concerns include processor data throughput and interaction between concurrently operating sensors (crosstalk).
2. Investigate loaded and unloaded classification algorithms within the trade space of erroneous prediction and processor firmware complexity, then demonstrate the ability to determine the loading status within the measurement time period allotted by a fast-moving train and confirm the processing is not too CPU-intense to be useful.
3. Refine the RFID/NFC firmware and determine maximum data extraction rates and connection distances from the TAG unit. Investigate inclusion/deletion of the internal SD card based upon the mission of the TAG unit – short-term engineering statistics or long-term physical property status.
4. Complete the development of the mechanical package and test for environmental and tamper vulnerabilities.
5. Conduct additional battery life testing to confirm anticipated power consumption during operation and sleep modes. The final packaging design is dependent on the size of battery that is required.
6. Conduct extensive field testing under various track conditions to verify operation and accuracy of the TAG units.

Abbreviations and Acronyms

AAS	Advanced Acoustics Sector
FRA	Federal Railroad Administration
GUI	Graphical User Interface
MCU	Micro Control Unit
MEMS	Micro-Electro-Mechanical Systems
NDEF	NFC Data Exchange Format
NFC	Near Field Communications
PN	Pennsylvania Northeastern Railroad
RF	Radio Frequency
RFID	Radio Frequency Identification
SD	Standard Digital
SEPTA	Southeastern Pennsylvania Transportation Authority
SRAM	Static Random-Access Memory